Assessment of Consolidation-Induced VOC Transport for a GML/GCL Composite Liner System

Hefu Pu, A.M.ASCE[1]; Charles D. Shackelford, F.ASCE[2]; and Patrick J. Fox, F.ASCE[3]

Abstract: This paper presents a numerical investigation of the effect of consolidation on the transport of a volatile organic compound (VOC), trichloroethylene (TCE), through a composite liner system comprising a geomembrane liner (GML) overlying and intimate contact with a geosynthetic clay liner (GCL). The numerical simulations were conducted using the model CST2, and considered coupled consolidation and contaminant transport with representative geometry, material properties, and applied stress conditions. The simulation results indicate that, depending on conditions, GCL consolidation can have significant effects on TCE mass flux, cumulative mass outflow, and distribution of contaminant concentration within the GCL, not only during the course of consolidation but also long after consolidation has ceased. Because of the small thickness of the GCL, consolidation-induced advection is insignificant. However, consolidation can significantly impact TCE transport through the GCL via changes in GCL material properties, including decreases in thickness, porosity, and effective diffusion coefficient. In general, the effects of GCL consolidation increase with increasing magnitude of applied stress, decreasing loading period (i.e., increasing loading rate), and increasing variation in the effective diffusion coefficient. The traditional performance assessment approach neglects GCL consolidation and fails to consider associated changes in material properties and, thus, can lead to significantly different results. Simulation results indicate that, in general, when the applied stress is lower than 125 kPa or the exponent for porosity-dependent effective diffusion coefficient is lower than 4, the effect of consolidation on TCE transport through the GML/GCL composite liner is insignificant, with differences in performance of the GML/GCL composite liner resulting from consolidation being less than 15%. **DOI: 10.1061/(ASCE)GT.1943-5606.0001538.**

Author keywords: Consolidation; Contaminant transport; Geosynthetic clay liner; Numerical modeling.

Introduction

Bottom liner systems are required for modern landfills to contain waste materials and control the release of hazardous chemicals to the surrounding environment. Such systems typically consist of a composite liner comprising a geomembrane liner (GML) overlying either a compacted clay liner (CCL) or a geosynthetic clay liner (GCL). A previous study focused on a numerical assessment of contaminant transport through the GML/CCL composite liner system (Pu et al. 2016). The focus of this study pertains to contaminant transport through a GML/GCL composite liner system, which is a popular alternative to the GML/CCL system, especially as the primary (top) liner in a double-composite liner system for containment of hazardous solid waste in accordance with the Resource Conservation and Recovery Act (RCRA) Subtitle C regulations (U.S. EPA 2014). Traditionally, modeling of contaminant transport through such systems is conducted using advective-diffusive models that assume the liners remain rigid during service life of the landfill (Shackelford 1990; Foose 2002). In reality, however, waste placement operations can occur over a long period of time and apply a significant vertical stress on the bottom liner system, such that the GCL will consolidate and, thus, produce transient advection and changes in material properties, which subsequently can affect the process of contaminant transport through the liner system. The question to be answered, then, is to what extent, if any, will the consolidation of the GCL affect the performance of the liner system?

Some studies have evaluated the effect of consolidation-induced contaminant transport for CCL-based liner systems, including field studies (Othman et al. 1997) and, more typically, numerical investigations (Peters and Smith 2002; Fox 2007b; Lewis et al. 2009; Zhang et al. 2013; Pu et al. 2016). These studies have shown that CCL consolidation can significantly affect the assessment of contaminant transport, including contaminant breakthrough time, mass flux, cumulative mass outflow, and contaminant distribution within the CCL. However, no study has been conducted to assess the effect, if any, of consolidation-induced contaminant transport for a GCL-based composite liner system.

This paper presents the results of a numerical investigation of the significance of consolidation-induced advection and changes of GCL material properties on the transport of trichloroethylene (TCE), a volatile organic compound (VOC) commonly encountered in landfill leachates (Lake and Rowe 2004), through a GML/GCL composite liner system with representative geometry, material properties, and applied stress conditions. The results of previous studies have shown that geomembranes formed from a single polymer (e.g., high-density polyethylene) typically provide little resistance to the diffusion of VOCs, such that containment of VOCs with GMLs is problematic (Edil 2003; Shackelford 2014). Numerical simulations were conducted using the CST2 numerical model for coupled large strain consolidation and transport as described by

[1]Professor, Institute of Geotechnical and Underground Engineering, Huazhong Univ. of Science and Technology, Wuhan, Hubei 430074, China (corresponding author). E-mail: puh@hust.edu.cn; hefupu85@gmail.com

[2]Professor and Head, Dept. of Civil and Environmental Engineering, Colorado State Univ., Fort Collins, CO 80523. E-mail: shackel@engr.colostate.edu

[3]Shaw Professor and Head, Dept. of Civil and Environmental Engineering, Pennsylvania State Univ., University Park, PA 16802. E-mail: pjfox@engr.psu.edu

Note. This manuscript was submitted on September 16, 2015; approved on March 21, 2016; published online on June 9, 2016. Discussion period open until November 9, 2016; separate discussions must be submitted for individual papers. This paper is part of the ***Journal of Geotechnical and Geoenvironmental Engineering***, © ASCE, ISSN 1090-0241.

Fox and Lee (2008). After describing the CST2 model, the results of numerical simulations using CST2 are compared on the basis of three baseline simulation cases, one of which includes the effect of GCL consolidation and the other two assume the GCL is rigid with constant properties. A parametric study then is presented to evaluate the effect of applied stress magnitude, loading period, and variation of effective diffusion coefficient on short-term and long-term transport of TCE through the GML/GCL composite liner system. Differences in the results are discussed, and a simplified method is proposed to partially compensate for the effects of GCL consolidation when analyzing VOC transport through a GML/GCL liner system.

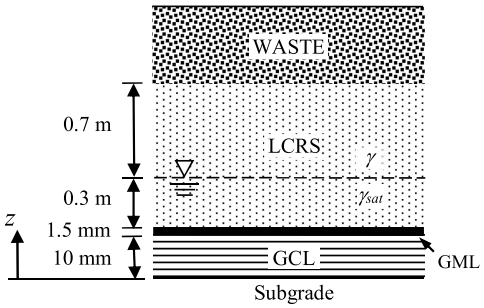

Fig. 1. Initial configuration for GML/GCL composite liner system

Numerical Model

CST2 is a numerical model for the simulation of coupled large strain consolidation and solute transport in saturated soil (Fox and Lee 2008). The consolidation algorithm for CST2 is based on the CS2 method (Fox and Berles 1997; Fox and Pu 2012), which accounts for vertical strain, soil self-weight, general constitutive relationships, relative velocity of fluid and solid phases, changing material properties during consolidation, time-dependent loading, unloading/reloading effects, and an external hydraulic gradient. Soil constitutive relationships are defined using discrete points and can take nearly any desired form. CST2 does not account for the effects of strain rate, secondary compression, or aging on the compressibility or hydraulic conductivity of the soil. The contaminant transport algorithm accounts for advection, diffusion, dispersion, equilibrium or nonequilibrium sorption, linear or nonlinear sorption, and an effective diffusion coefficient that changes with soil porosity. Contaminant transport is consistent with temporal and spatial variations of porosity and seepage velocity. Depending on parameter values, CST2 can simulate diffusion-controlled, advection-controlled, or combined advective-diffusive contaminant transport (Fox 2007b). The key to the transport algorithm is the definition of two Lagrangian fields of elements that separately follow the motions of solid and fluid phases. This approach reduces numerical dispersion and simplifies transport calculations to dispersion mass flow between contiguous fluid elements (Fox 2007a). Transport conditions for the top and bottom boundaries can be prescribed concentration (Type I), prescribed concentration gradient (Type II), or prescribed solute mass flux (Type III). CST2 can also accommodate a reservoir boundary, which represents an accumulating well-mixed aqueous reservoir formed by fluid outflow at the top boundary. The CST2 model and its predecessors have undergone extensive validation, including comparisons with experimental data (e.g., Fox and Berles 1997; Fox 2007b; Fox and Lee 2008; Lee and Fox 2009; Fox and Pu 2015).

Numerical Simulations

Baseline Conditions

Liner System

Baseline simulation conditions, which use representative material and transport properties and stress conditions, are defined first as the basis for the subsequent parametric study. The initial configuration is shown in Fig. 1. The GML/GCL composite liner system consists of, from bottom to top, a subgrade layer, GCL, GML, and leachate collection and removal system (LCRS). The subgrade can represent an underlying leachate detection system (LDS) typical of double-composite liner systems for hazardous waste containment, or a natural soil layer at atmospheric pore pressure, and is assumed to be drained. The GCL has an initial thickness H_o of 10 mm (Shackelford et al. 2000) with the vertical coordinate z directed upward from the base. The GML is an intact, 1.5-mm-thick high-density polyethylene (HDPE) geomembrane that is in intimate contact with the top surface of the GCL, i.e., zero GML/GCL interface transmissivity (Harpur et al. 1993; Mendes et al. 2010). The LCRS has a constant thickness of 1 m. The top boundary of the GCL is assumed to be undrained, which is reasonable because, as shown by Harpur et al. (1993) and Mendes et al. (2010), the geotextile component is essentially nonconductive in the in-plane direction due to extrusion of bentonite into the geotextile. The GML is subjected to a constant leachate height of 0.3 m from the overlying LCRS.

The leachate contains a VOC at a constant concentration c_o of 100 mg/L, which is assumed to be sufficiently dilute so as to not alter material properties of the GCL. The GCL is initially uncontaminated and the concentration at the bottom of the GCL is maintained at zero ($c = 0$) for all times. This lower boundary condition allows for diffusion across the interface and produces the highest (i.e., most conservative) estimate of contaminant mass flux (Rabideau and Khandelwal 1998; Foose 2002; Pu and Fox 2015). Although semipermeable membrane effects (e.g., solute restriction, chemico-osmosis) can be significant for engineered barriers composed of high swelling smectite minerals, such as sodium bentonite in the GCL (Shackelford 2011, 2013), these effects are neglected, which is also conservative from a transport standpoint. VOC transport through GML holes is also neglected because mass flux by leakage through GML holes is much smaller than mass flux through the intact area of a GML by diffusion (Foose et al. 2002; Shackelford 2014). As a result, the VOC first diffuses through the intact GML prior to reaching the GCL, and then undergoes advective-diffusive transport through the GCL with sorption onto the bentonite and geotextiles components of the GCL.

Material and Transport Properties

Material properties for the GCL were taken from experimental data reported by Kang and Shackelford (2010). In that study, the bentonite component of the GCL contained 71% smectite (montmorillonite), 7% mixed layer illite/smectite, 15% quartz, and 7% other minerals. The measured liquid limit and plastic limit [ASTM D4318 (ASTM 2010a)] were 478 and 39, respectively, and the bentonite was classified as CH (high plasticity clay) based on the Unified Soil Classification System [ASTM D2487 (ASTM 2011)]. The compressibility and hydraulic conductivity constitutive relationships, which were obtained for duplicate specimens of the GCL (i.e., GCL1 and GCL2), are shown in Fig. 2. The compressibility relationships display trends similar to natural normally consolidated soils, with a compression index C_c of 1.31 for GCL1 and 1.57 for GCL2. The average compressibility relationship based on those for GCL1 and GCL2 is used in this study, and is expressed as

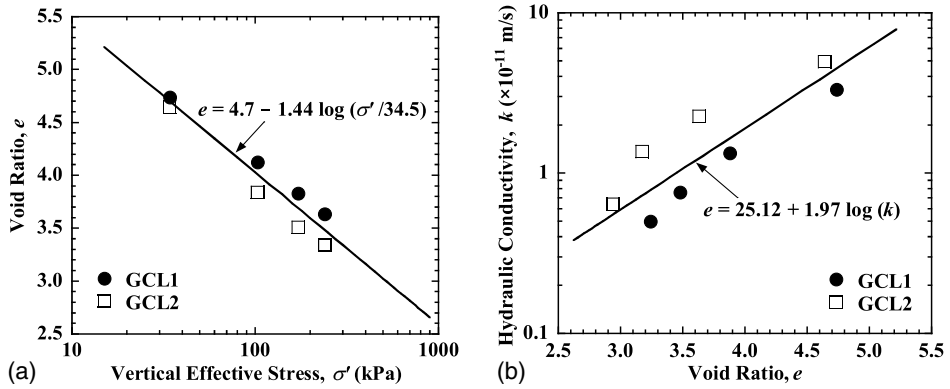

Fig. 2. Constitutive relationships for GCL: (a) compressibility; (b) hydraulic conductivity (data points from Kang and Shackelford 2010)

$e = 4.7 - 1.44\log(\sigma'/34.5)$, where e = void ratio and σ' = vertical effective stress (kPa). Hydraulic conductivity was measured after each load increment in general accordance with procedures of ASTM D5084 (ASTM 2010b). In this study, the average hydraulic conductivity relationship of GCL1 and GCL2 is used, and is expressed as $e = 25.12 + 1.97\log(k)$, where k = vertical hydraulic conductivity (m/s). Both compressibility and hydraulic conductivity relationships change nonlinearly with void ratio; thus, the coefficient of consolidation also will change nonlinearly during the consolidation process.

Numerical simulations were conducted for transport of TCE. TCE transport properties for nonsorbing and sorbing GCLs, as reported by Yaws (1995), Rabideau et al. (1996), Kim et al. (2001), Lake and Rowe (2004), and Sleep et al. (2006), are presented in Table 1. The effective diffusion coefficient D^* varies with porosity n in the form $D^* = D_o n^M$, where D_o = free solution (aqueous phase) diffusion coefficient and M = empirical exponent (Manheim 1970; Lerman 1978). Although values of M have been reported for a variety of porous media, including sediments, sands, and kaolinite clays (Lerman 1978; Ullman and Aller 1982; Parker et al. 1994; Boving and Grathwohl 2001; Lee et al. 2009), values of M for GCLs are scarce in the literature. The base value for M of 8.67 used in the current study was calculated from values of D_o ($= 8.6 \times 10^{-10}$ m^2/s), D^* ($= 2.1 \times 10^{-10}$ m^2/s), and n (= 0.85) reported for TCE by Lake and Rowe (2004). Mechanical dispersion is assumed to be negligible (i.e., $\alpha_L = 0$) because of the small thickness of the GCL and low values of the seepage velocity v_s typically associated with GCLs due, in part, to the low hydraulic conductivity (e.g., Rabideau et al. 1996; Sleep et al. 2006; Mitchell et al. 2007). Diffusive mass flux through the GML is characterized using Fick's first law and corresponds to a variable flux boundary condition at the top of the GCL (Fox 2007b; Pu 2014). Values for the GML diffusion coefficient D_{GML} of 4×10^{-13} m^2/s and the GML partition coefficient K_{GML} of 85 were taken from experimental data reported by Sangam and Rowe (2001).

Table 1. TCE Transport Properties for GCL in Baseline Simulation Conditions

Property	Nonsorbing GCL	Sorbing GCL
Free solution diffusion coefficient D_o ($\times 10^{-10}$ m^2/s)	8.6[a]	8.6[a]
Exponent for effective diffusion coefficient M	8.67[b]	8.67[b]
Longitudinal dispersivity α_L (m)	0[c]	0[c]
Distribution coefficient K_{dGCL} (mL/g)	0	7.94[d]

[a]Kim et al. (2001) and Yaws (1995).
[b]Lake and Rowe (2004).
[c]Rabideau et al. (1996) and Sleep et al. (2006).
[d]Eq. (1).

TCE sorption in the GCL is characterized using a linear equilibrium sorption isotherm with an equivalent distribution coefficient K_{dGCL} that includes TCE sorption to both the bentonite and the geotextile components of the GCL. The value of K_{dGCL} was calculated as a mass-based weighted average as follows (Mendes et al. 2013)

$$K_{dGCL} = \frac{K_{dBENT} M_{BENT} + K_{dGTX} M_{GTX}}{M_{BENT} + M_{GTX}} \quad (1)$$

where M_{BENT} ($= 4.5$ kg/m^2) and M_{GTX} ($= 0.62$ kg/m^2) are the dry masses of bentonite and geotextiles per unit area of the GCL, respectively, and K_{dBENT} ($= 0.9$ mL/g) and K_{dGTX} ($= 59$ mL/g) are the distribution coefficients for bentonite and geotextiles, respectively. These parameter values are based on experimental data reported by Lake (2000), Lake and Rowe (2004), Kolstad et al. (2004), Malusis and Scalia (2007), and Katsumi et al. (2008). For these values, Eq. (1) gives $K_{dGCL} = 7.94$ mL/g. With the assumption of linear equilibrium sorption, the retardation factor is expressed as $R_f = 1 + \rho_{dGCL} K_{dGCL}/n_{GCL}$, where n_{GCL} is the bulk porosity of GCL, ρ_{dGCL} is the equivalent dry density of GCL expressed as $\rho_w G_{sGCL}/(1 + e_{GCL})$, where ρ_w is the density of water, e_{GCL} is the bulk void ratio of GCL, and G_{sGCL} is the equivalent specific gravity of solids of the GCL and equal to 2.21, which was calculated as a harmonic mean of the constituent values of G_s, i.e., 2.74 for the GCL bentonite (Castelbaum and Shackelford 2009) and 0.91 for the GCL geotextile (Lake 2000). To illustrate the effect of sorption, a nonsorbing GCL is also considered in this study (i.e., $K_{dGCL} = 0$). For both nonsorbing and sorbing GCLs, TCE decay due to biological processes is neglected, which is conservative.

Stress Conditions

Initial stress conditions are calculated assuming the GCL is saturated. This assumption is conservative in terms of mass transport (i.e., results in a greater mass flux) and also reasonable from the standpoint that prehydrated GCLs are desired in order to eliminate suction within the GCL and to develop full swelling potential of the bentonite so as to minimize the hydraulic conductivity of the GCL (Shackelford et al. 2000; Lee and Shackelford 2005; Shackelford 2005). For the LCRS layer, the saturated unit weight $\gamma_{sat} = 20.6$ kN/m^3 for the lower 0.3 m and moist unit weight $\gamma = 17.5$ kN/m^3 for the upper 0.7 m. Under these conditions, and neglecting the weight of the GML but assuming full capillary rise in the GCL under a hydrostatic condition, the initial vertical effective

stress at the top of the GCL is $q_o = 0.7\gamma + 0.3\gamma_{sat} + H_o\gamma_w = 18.5$ kPa. Starting at time $t = 0$, the applied vertical stress increases at a constant rate to final value Δq over the landfill loading period t_q and remains constant thereafter. The total elapsed time for each simulation is 40 years. CST2 simulations were conducted using 100 solid elements, 100 fluid elements for simulations without GCL sorption, and 300 fluid elements for simulations with GCL sorption. These levels of numerical resolution are expected to yield results of high accuracy (Fox 2007b).

Simulation Cases

Three types of simulation cases were conducted to illustrate differences in TCE transport with and without the effect of GCL consolidation. The first type of simulation case, denoted as C, considers fully coupled consolidation and transport. The second type of simulation case, denoted as NC-I (i.e., No Consolidation-Initial), ignores GCL consolidation ($\Delta q = 0$) and is conducted using initial conditions of the liner system held constant over the 40-year simulation period (i.e., constant initial GCL thickness and constant initial profiles of void ratio and effective diffusion coefficient). The third type of simulation case, denoted as NC-F (i.e., No Consolidation-Final), also ignores GCL consolidation ($\Delta q = 0$), but is conducted using final conditions of the liner system held constant over the 40-year simulation period (i.e., constant final GCL thickness and constant final profiles of void ratio and effective diffusion coefficient). As such, conditions for the NC-I and NC-F simulation cases represent the initial and final conditions for the C simulation case, respectively, and are conducted to provide a reference for comparison of the results with those for the C simulation case. For the C simulation case, although GCL transport properties are constant (Table 1), consolidation-induced spatial and temporal changes in porosity and seepage velocity produce variations of advection, dispersion, and sorption. These variations represent major differences between the C simulation case versus the NC-I and NC-F simulation cases. For the NC-I and NC-F simulation cases, in contrast, consolidation is ignored such that TCE transport occurs only by diffusion (e.g., Shackelford 2014).

All simulation cases (C, NC-I, NC-F) were conducted using the CST2 model with appropriate input parameters. Parameter values for each baseline simulation case are summarized in Table 2. C and NC-I simulation cases were conducted with $H_o = 10$ mm and NC-F simulations were conducted with $H_o = 5.9$ mm. Total hydraulic head at the top and bottom boundaries of the GCL, h_t and h_b, respectively, are zero except for case C during consolidation, whereas initial effective stress at the top boundary of the GCL q_o varies with conditions. For C simulation case, the liner system is loaded at a constant rate of 100 kPa/year for a loading period t_q of 10 years, giving a final applied stress of 1,000 kPa. This waste loading corresponds to a municipal solid waste landfill with a 10-year filling period, a final waste height of approximately 70 to 90 m (Zekkos et al. 2006), and a 30-year postclosure period (Mitchell et al. 2007). No consolidation occurs for the NC-I and NC-F cases ($\Delta q = 0$). For all baseline simulations, M is 8.67. Table 2 also provides the values for initial void ratio e_o [calculated according to q_o and compressibility relationship in Fig. 2(a)], initial hydraulic conductivity k_o [calculated according to e_o and hydraulic conductivity relationship in Fig. 2(b)], and initial effective diffusion coefficient D_o^* (calculated according to e_o and D^* versus n relationship) for each simulation case.

Parametric Study

Following the baseline simulations, a parametric study was conducted to investigate the effect of several variables on TCE transport through the GML/GCL liner system. These variables are applied stress magnitude, loading period, and effective diffusion coefficient. For each series of simulations, only the variable of interest was changed, while other variables were held constant and equal to those for the respective baseline case.

Table 2. Baseline Parameter Values for the Three Simulation Cases (C = Consolidation; NC-I = No Consolidation-Initial; NC-F = No Consolidation-Final)

Parameter	Value		
	C	NC-I[a]	NC-F[b]
H_o (mm)	10	10	5.9
h_t (mm)	0[c]	0	0
h_b (mm)	0	0	0
q_o (kPa)	18.5	18.5	1,018.5
Δq (kPa)	1,000	0	0
t_q (years)	10	0	0
M	8.67	8.67	8.67
e_o	5.09	5.09	2.58
D_o^* ($\times 10^{-10}$ m^2/s)	1.815	1.815	0.504
k_o ($\times 10^{-11}$ m/s)	6.80	6.80	0.36

[a]Conditions for NC-I are equal to initial conditions for C.
[b]Conditions for NC-F are equal to final conditions for C.
[c]Initial and final conditions only.

Simulation Results

Baseline Conditions

Values of applied stress Δq and GCL compression ΔH for the C simulations of the GML/GCL system are presented in Fig. 3(a). Consolidation is completed immediately after the end of the loading period ($t = 10$ years) due to the small thickness of the GCL, and the resulting final compression of the GCL is 4.1 mm, which corresponds to the final vertical strain of 41%. Pu et al. (2016) presented the results of a similar numerical investigation of consolidation-induced VOC transport for a GML/CCL composite liner system, in which a GML with the same properties as those in the current study was underlain by a 1-m-thick, low-compressibility CCL. With the same loading schedule and boundary conditions, the final vertical strain for the CCL was significantly lower and equal to 9.4%. Thus, the final vertical strain for the GCL in this study is much higher than for the CCL because the GCL bentonite is more compressible than the CCL clay. The initial and final void ratios for the GCL are 5.09 and 2.58, respectively. Based on this change in void ratio, the value of D^* for the GCL decreases by 72% as a result of consolidation.

The water outflow rate v at the bottom boundary for the C simulation of the GML/GCL system is presented in Fig. 3(b). The value of v for the GCL is relatively high at the start of loading, but gradually decreases as excess pore-water pressures dissipate, and then rapidly decreases to zero immediately after the end of loading (i.e., $t = 10$ years). A sudden decrease occurs in Fig. 3(b) at $t = 10$ years because the transition of outflow rate from a nonzero value at the end of the loading period ($t = 10$ years) to a steady-state zero value requires less than 1 day due to the small thickness of the GCL, i.e., short drainage distance. The maximum value of v for the GML/GCL is approximately 5 mm/year, which is much lower than that for the GML/CCL (i.e., 30 mm/year) presented by Pu et al. (2016). This much lower outflow rate occurs for the GML/GCL because the 10-mm-thick GCL is much thinner than 1-m-thick CCL and the hydraulic conductivity of the GCL is much lower than that of the CCL.

Simulation results for TCE transport through the GML/GCL system for baseline conditions over the 40-year simulation period

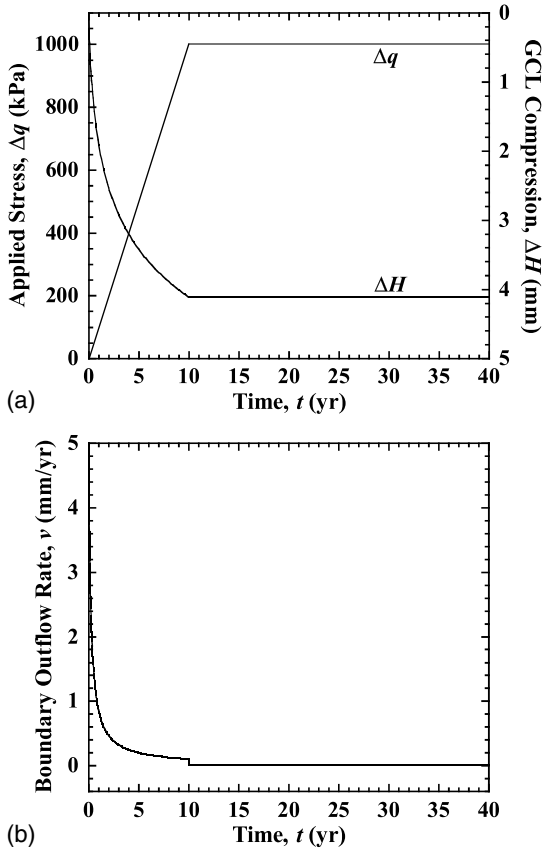

Fig. 3. Consolidation response for GML/GCL composite liner: (a) applied stress and GCL compression; (b) bottom boundary water outflow rate

are presented in Fig. 4, and include (1) TCE mass flux F, (2) TCE advective mass flux versus diffusive mass flux, (3) normalized TCE mass flux F/F_{ss}, and (4) cumulative TCE mass outflow per unit area M_e at the bottom of the GCL. Values of final steady-state mass flux F_{ss} were calculated using the analytical solution presented by Foose et al. (2002) and are equal to those from the CST2 simulations. For the nonsorbing GCL ($K_{dGCL} = 0$), Fig. 4(a) indicates that TCE breakthrough for the NC-I and NC-F simulations occurs almost immediately and reaches steady state within a few days. Steady-state mass flux for the NC-I simulations is 87% higher than that for the NC-F simulations because D^* for the NC-I simulations is much higher. TCE mass flux for the C simulations is the same as that for the NC-I simulations in the very early stages ($t < 0.04$ year), and then decreases with elapsed time due to consolidation-induced reduction in D^*, and ultimately becomes the same as that for the NC-F simulations immediately after the end of consolidation ($t = 10$ years). The NC-F simulations provide the same estimate of long-term mass flux as the C simulations because the NC-F simulations partially take into account the consolidation effect by using final values of GCL thickness, n, and D^*. The trends of the simulation results for a sorbing GCL ($K_{dGCL} > 0$) are essentially the same as those for the nonsorbing GCL, which is attributed to the minimal mass of soil solids available for TCE sorption due to the small thickness of the GCL. Thus, the effect of sorption in the GCL is minimal for the conditions simulated.

To illustrate the respective contribution of advection and diffusion, Fig. 4(b) presents advective mass flux, diffusive mass flux, and total mass flux for the C simulations during the 10-year consolidation period. Total mass flux is the sum of advective mass flux and diffusive mass flux, and is equal to the mass flux shown in Fig. 4(a). Fig. 4(b) indicates that the advective mass flux is essentially zero throughout the consolidation period, with a maximum value of less than 0.001 mg/m^2/year occurring at approximately

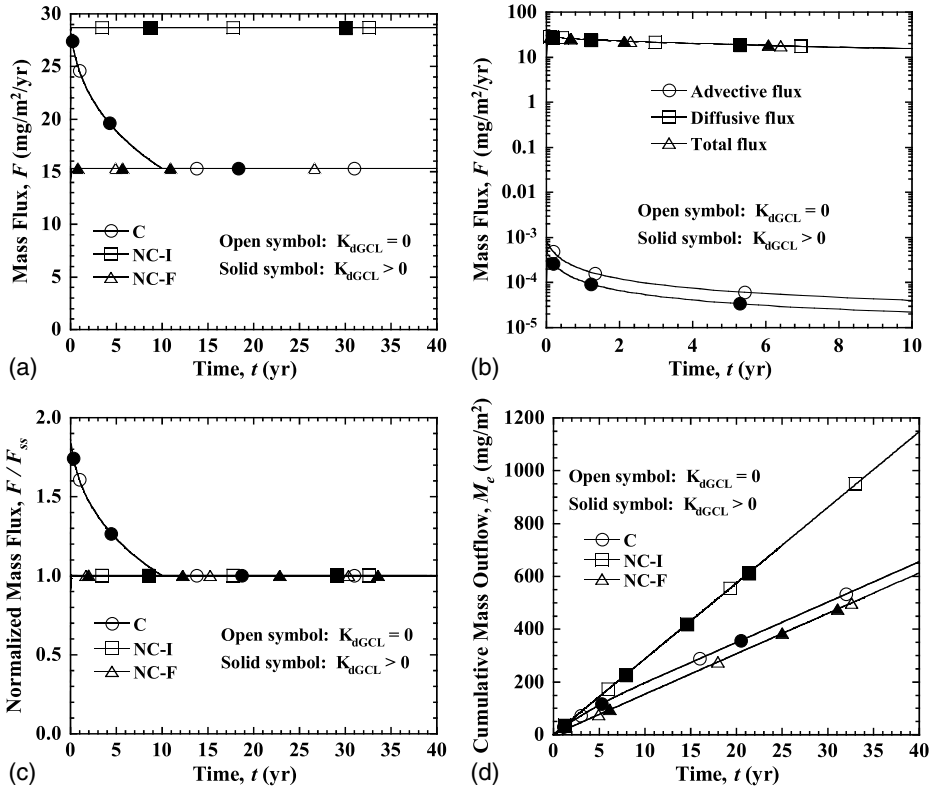

Fig. 4. Simulation results for GML/GCL composite liner: (a) TCE mass flux; (b) TCE advective mass flux versus diffusive mass flux for case C; (c) normalized TCE mass flux; (d) cumulative TCE mass outflow

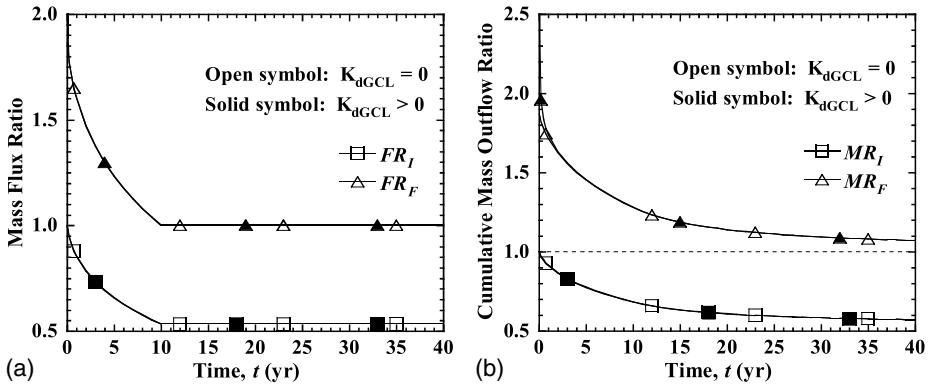

Fig. 5. Ratios of simulation results: (a) TCE mass flux ratio; (b) cumulative TCE mass outflow ratio

$t = 12$ days. In contrast, the diffusive mass flux is at least five orders of magnitude higher than the advective mass flux such that the total mass flux is almost entirely attributed to diffusion. Consolidation-induced advective transport is negligible because of the small thickness and low hydraulic conductivity of the GCL such that the consolidation-induced water flow rate is negligible.

Temporal relationships for F/F_{ss} are shown in Fig. 4(c) and indicate that all three simulation cases (C, NC-I, NC-F) for both nonsorbing and sorbing GCLs reach steady state. Interestingly, F/F_{ss} values for the C simulations are greater than unity ($F/F_{ss} > 1.0$) during the consolidation period ($t < 10$ years), which is attributed to a higher D^* value during consolidation relative to the final D^* value at steady state. Temporal trends in M_e are shown in Fig. 4(d). As the slopes in these trends are proportional to the values of F in Fig. 4(a), the relative differences in the simulations cases in Fig. 4(d) are the same as those in Fig. 4(a). Thus, for both nonsorbing and sorbing GCLs, values of M_e for the C simulations tend to be intermediate between those for the NC-F and NC-I simulations, with M_e values for the C simulations being initially the same as those for the NC-I simulations, but then gradually decreasing towards limiting values for the NC-F simulations after the end of consolidation ($t > 10$ years).

The effect of GCL consolidation on contaminant transport is indicated in Fig. 5 using two ratios for contaminant mass flux [i.e., Fig. 5(a)], and two ratios for cumulative mass outflow [i.e., Fig. 5(b)]. The mass flux ratios are denoted as FR_I ($=F_C/F_{\text{NC-I}}$) and FR_F ($=F_C/F_{\text{NC-F}}$), where F_C, $F_{\text{NC-I}}$, and $F_{\text{NC-F}}$ are values of mass flux at any time for C, NC-I, and NC-F simulations, respectively. Likewise, the cumulative mass outflow ratios are denoted as MR_I ($=M_{e,C}/M_{e,\text{NC-I}}$) and MR_F ($=M_{e,C}/M_{e,\text{NC-F}}$), where $M_{e,C}$, $M_{e,\text{NC-I}}$, and $M_{e,\text{NC-F}}$ are values of cumulative mass outflow for C, NC-I, and NC-F simulations. Fig. 5(a) indicates that, for both nonsorbing and sorbing GCLs, values of FR_I are initially 1.0, then decrease with elapsed time, and ultimately become approximately 0.5 after the end of consolidation, which indicates that the NC-I simulations overestimate the long-term mass flux by a factor of approximately 2. F_C values are consistently lower than $F_{\text{NC-I}}$ values because consolidation-induced advective transport for the C simulations is negligible and consolidation-induced changes in GCL properties (e.g., 72% reduction in D^*) decreases the F_C values throughout the simulation period. During the consolidation period, this lower F_C relative to $F_{\text{NC-I}}$ for GML/GCL is in contrast to the results for GML/CCL presented by Pu et al. (2016), where F_C in the early stages is as high as 10 times $F_{\text{NC-I}}$ for nonsorbing CCL because the CCL is much thicker than the GCL and the hydraulic conductivity of the CCL is much higher than that of the GCL, such that consolidation-induced advection is more significant for a CCL-based composite liner. Fig. 5(a) also indicates that values of FR_F are greater than 1.0 during consolidation, decrease to 1.0 immediately after the end of consolidation, and are the same for nonsorbing and sorbing GCLs. The value of D^* for the NC-F simulations is lower than that for the C simulations during consolidation, which yields lower values of $F_{\text{NC-F}}$. The NC-F simulations provide the same value of long-term mass flux as the C simulations because the NC-F simulations partially take into account the effect of consolidation by using the final (i.e., after consolidation) values of D^*, n, and GCL thickness. The corresponding MR_I and MR_F relationships, shown in Fig. 5(b), indicate similar trends, with NC-I simulations yielding higher long-term M_e values and NC-F simulations yielding similar long-term M_e values relative to the C simulations.

Fig. 6 presents profiles of relative TCE concentrations c/c_o for the GML/GCL system with a nonsorbing GCL at $t = 1$ day, 5 years, and 10 years. At the early time ($t = 1$ day), concentrations at any elevation for the C simulation are equal to those for the NC-I simulation because consolidation-induced downward advection and changes in GCL properties are both negligible at the beginning of consolidation. The concentration profiles at $t = 1$ day are nonlinear for both C and NC-I, indicating a transient state due to insufficient elapsed time for diffusion. At later times for the NC-I simulations, the profile at $t = 5$ years is linear and equal to that at $t = 10$ years, indicating final steady-state diffusive transport. In contrast, for the C simulations, the profile at $t = 5$ years is also linear but has not reached final steady state due to ongoing consolidation during the 10-year loading period, whereas the profile at $t = 10$ years reaches final steady-state diffusive transport due to completion of consolidation and sufficient time for diffusion. Final steady-state profiles calculated using the analytical solution of

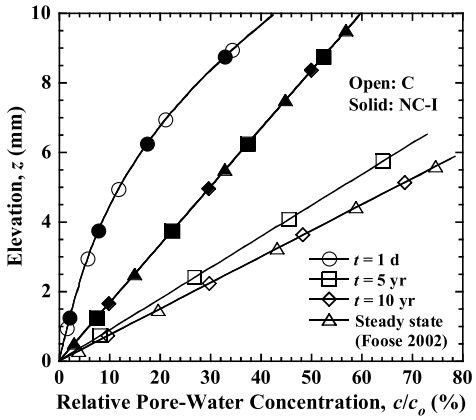

Fig. 6. TCE concentration profiles for nonsorbing GCL within GML/GCL composite liner

Foose (2002) are also shown in Fig. 6 and are the same as the corresponding profiles from CST2. Final concentrations for the C simulations are higher than those for the NC-I simulations at any elevation due to changes in GCL properties for the C simulations. Corresponding concentration profiles for the sorbing GCL (not shown) display essentially the same trends as for the nonsorbing GCL, which is consistent with the mass flux curves in Fig. 4. Profiles for relative solid-phase concentration s/s_o (not shown), where $s_o = K_{\text{dGCL}} c_o$, also display the same trends as a result of linear equilibrium sorption.

Parametric Study

Applied Stress Magnitude

To investigate the effect of applied stress magnitude on TCE transport through the GML/CCL system, simulations were conducted for baseline conditions with $\Delta q = 125$, 250, 500, and 1,000 kPa. For these Δq values, the resulting final GCL vertical strains are 21%, 27%, 34%, and 41%, respectively, and the corresponding reductions in D^* are 37%, 49%, 61%, and 72%. Fig. 7 presents temporal relationships for MR_I and MR_F with varying Δq. For all simulations, MR_I values are initially 1.0 and decrease with elapsed time, and indicate that the consolidation effect becomes more significant with increasing Δq. At the end of the 40-year simulation period, the NC-I simulations overestimate TCE mass outflow by 15, 22, 31, and 43% for Δq of 125, 250, 500, and 1,000 kPa, relative to the respective C simulations. Increasing the applied stress magnitude results in more compression, and thus produces greater changes in GCL transport properties. Fig. 7(a) also indicates that the MR_I values are essentially the same for the nonsorbing and sorbing GCLs because the mass of soil solids available for TCE sorption is minimal and, thus, the retardation effect is negligible for the GCL. In contrast, the values of MR_F shown in Fig. 7(b) are greater than 1.0, indicating that the NC-F simulations underestimate TCE mass outflow relative to C simulations for all simulations. The MR_F values decrease with time and approach approximately 1.0 near the end of the simulation period, indicating that the NC-F simulations provide a similar estimate of long-term TCE mass outflow as the C simulations for varying Δq.

Loading Period

To investigate the effect of loading period on TCE transport through the GML/GCL system, simulations were conducted for baseline conditions with $t_q = 0$, 10, and 20 years, where $t_q = 0$ represents instantaneous waste placement. Fig. 8 presents temporal relationships for MR_I and MR_F with varying t_q. The values of MR_I and MR_F consistently decrease with decreasing loading period (i.e., increasing loading rate) because a more rapid change of GCL properties occurs for the C simulations, such that the associated contaminant mass flux decreases. The MR_I values are less than 1.0 and essentially equal for nonsorbing and sorbing GCLs, and the consolidation effect is more significant for a shorter loading period. For $t_q = 0$ year, for example, MR_I values are approximately 0.5 throughout the 40-year simulation period; thus, the NC-I simulations overestimate TCE mass outflow by a factor of approximately 2. The MR_F values generally exceed 1.0 during the early stages but approach 1.0 near the end of the simulation period. In general, t_q has an important effect during the early stages but a lesser effect toward the end of each simulation period because t_q affects the rate of consolidation but not the final vertical strain or final material properties of the GCL.

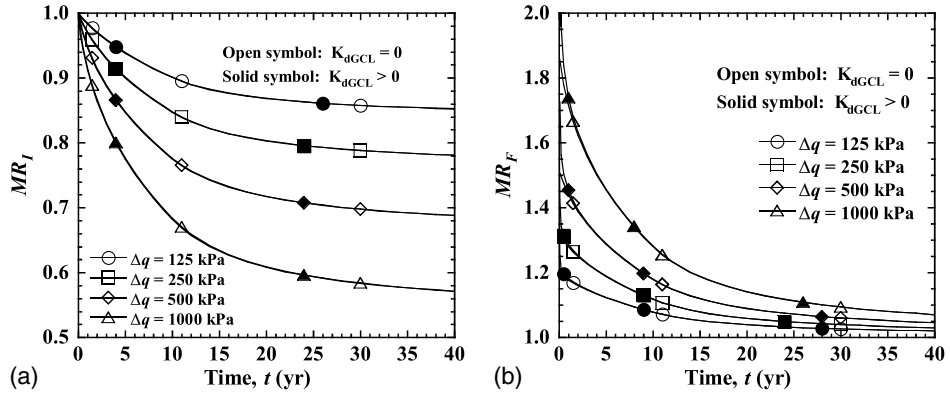

Fig. 7. Cumulative TCE mass outflow ratios for varying applied stress magnitude: (a) MR_I; (b) MR_F

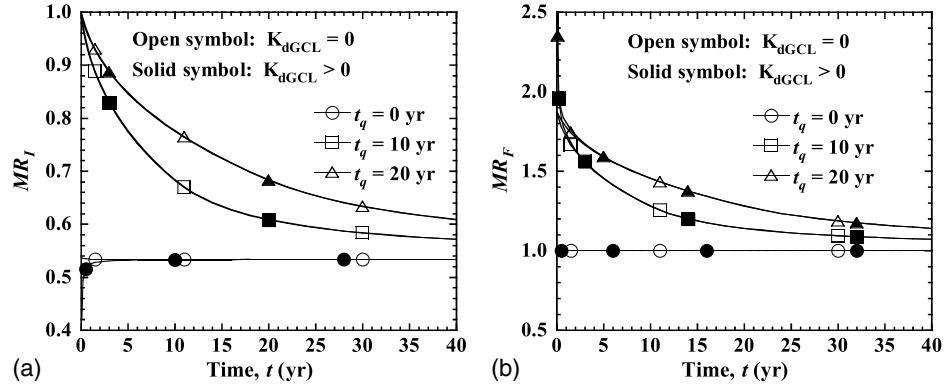

Fig. 8. Cumulative TCE mass outflow ratios for varying loading period: (a) MR_I; (b) MR_F

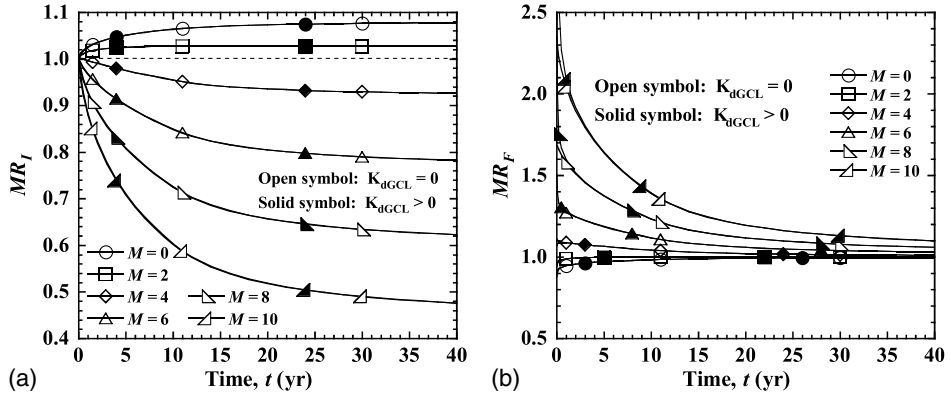

Fig. 9. Cumulative TCE mass outflow ratios for varying exponent M: (a) MR_I; (b) MR_F

Effective Diffusion Coefficient

To investigate the effect of variation of D^* on TCE transport through the GML/GCL system, simulations were conducted for baseline conditions with $D^* = D_o n^M$ and $M = 0, 2, 4, 6, 8$, and 10, where $M = 0$ represents constant D^*. For these M values, the consolidation-induced reductions in D^* are 0, 26, 45, 59, 69, and 77%, respectively. Fig. 9 presents temporal relationships for MR_I and MR_F with varying M. The MR_I values are initially 1.0 for all simulations, and decrease with elapsed time for $M \geq 4$ but increase with elapsed time for $M \leq 2$. The simulations also generally indicate that the consolidation effect is more significant for high M values because the change in D^* for a given change in n increases as M increases. Depending on the value of M, the NC-I simulations can either overestimate or underestimate TCE mass outflow relative to the C simulations. For $M \geq 4$, the NC-I simulations overestimate TCE mass flux because consolidation causes a more significant reduction in D^* for higher M values for the C simulations. The effect of consolidation is the greatest for $M = 10$, where NC-I simulations overestimate TCE mass flux by 52% at $t = 40$ years. For $M \leq 2$, in contrast, the NC-I simulations underestimate TCE mass flux because consolidation causes only a slight reduction in D^* for lower M values. In this case, the consolidation-induced reduction in transport distance H (i.e., 41% reduction) is more dominant, such that the C simulations produce higher mass flux. For $M = 0$, the NC-I simulations underestimate TCE mass flux by 8% at $t = 40$ years. Fig. 9(a) again indicates that MR_I values are essentially equal for the nonsorbing and sorbing GCLs for all M values such that the retardation effect is negligible for the GCL. Values of MR_F, shown in Fig. 9(b), are greater than 1.0 for $M \geq 4$ and slightly less than 1.0 for $M \leq 2$ during the early stages, with nonsorbing and sorbing GCLs indicating only slightly different values, but approach 1.0 near the end of the simulation period for all conditions. These trends suggest that, for the M values considered, the NC-F simulations provide a similar estimate of long-term TCE mass outflow as the C simulations.

Conclusions

The following conclusions result from the foregoing numerical investigation of consolidation-induced transport of the volatile organic compound trichloroethylene (TCE) through a landfill bottom liner system consisting of a geomembrane liner (GML) overlying and in intimate contact with a geosynthetic clay liner (GCL):

1. Depending on material properties and conditions (e.g., loading conditions, initial and boundary conditions), GCL consolidation can have a significant effect on TCE transport through a GML/GCL composite liner system both during and long after the consolidation stage. As a result of the small thickness and low hydraulic conductivity of the GCL, consolidation-induced advection is shown to be insignificant. Nonetheless, consolidation can still have a significant effect on transport through the GML/GCL system, because the consolidation process changes GCL properties, including the thickness, void ratio, and effective diffusion coefficient. For the baseline conditions considered, consolidation causes a reduction of 41, 49, and 72% in GCL thickness, void ratio, and effective diffusion coefficient, respectively, and, as a result, a reduction of 47% and 43% in final steady-state TCE mass flux and cumulative TCE mass outflow at the bottom of the GCL relative to results for traditional diffusive simulations that neglect consolidation of the GCL.
2. Simulations for TCE transport were conducted for three cases, the C, NC-I, and NC-F cases. The C simulations corresponded to fully coupled consolidation and transport. The NC-I and NC-F simulations corresponded to constant initial conditions (before consolidation) and constant final conditions (after consolidation), respectively, for the GCL over the entire simulation period. The NC-I and NC-F simulations did not consider the effect of coupled consolidation and transport and, thus, yielded significantly different results for TCE mass flux, cumulative TCE mass outflow, and fluid-phase and solid-phase TCE concentration distributions. Depending on conditions, the NC-I simulations either overestimate or underestimate transport results relative to the C simulations. The NC-I simulations overestimate the transport results for $M \geq 4$ and underestimate the transport results for $M \leq 2$, where M is an exponent that accounts for a porosity-dependent effective diffusion coefficient. For $M = 10$, the NC-I simulation overestimates cumulative TCE mass outflow by 52%. In contrast, for $M = 0$, the NC-I simulation underestimates cumulative TCE mass outflow by 8% at the end of simulation period ($t = 40$ years). NC-F simulations also either overestimate or underestimate transport during consolidation, but generally yield similar estimates of long-term TCE transport relative to the C simulations because the NC-F simulations account for consolidation-induced changes in the GCL thickness and material properties and, thus, partially account for the consolidation effect.
3. For the conditions simulated, the effect of GCL consolidation on TCE transport increases with increasing magnitude of applied stress, decreasing loading period (i.e., increasing loading rate), and increasing variation of effective diffusion coefficient with bentonite porosity. Each of these variables has a significant effect on TCE transport through a GML/CCL liner system.

4. For the conditions simulated, when the applied stress is lower than 125 kPa or the exponent M is lower than 4, consolidation-induced TCE transport through the GML/GCL liner system is insignificant, with differences resulting from consolidation being less than 15%. However, when the applied stress is greater than 125 kPa or the exponent M is greater than 4, the effect of GCL consolidation on TCE transport through the GML/GCL liner system is significant, primarily because of the change in transport properties for the GCL.

Acknowledgments

Financial support for this research was provided by the U.S. National Science Foundation (NSF), Arlington, VA, under Grant No. CMMI-1001023, Grant No. CMMI-0969346, and Grant No. CMMI-1363230. This support is gratefully acknowledged. The opinions expressed in this paper are solely those of the authors and are not necessarily consistent with the policies or opinions of the NSF.

Notation

The following symbols are used in this paper:

C = simulation that considers fully coupled consolidation and transport;
C_c = compression index;
c = fluid-phase contaminant concentration;
c_o = contaminant concentration in leachate;
e = void ratio;
e_o = initial void ratio;
D_{GML} = diffusion coefficient for GML;
D_h = hydrodynamic dispersion coefficient;
D_o = free solution diffusion coefficient;
D^* = effective diffusion coefficient;
D_o^* = initial effective diffusion coefficient;
F = contaminant mass flux per unit area at bottom of GCL;
F_C = contaminant mass flux per unit area for C case;
$F_{\mathrm{NC\text{-}I}}$ = contaminant mass flux per unit area for NC-I case;
$F_{\mathrm{NC\text{-}F}}$ = contaminant mass flux per unit area for NC-F case;
F_{ss} = steady-state contaminant mass flux per unit area at bottom of GCL;
FR_F = ratio of contaminant mass flux for C case to that for NC-F case;
FR_I = ratio of contaminant mass flux for C case to that for NC-I case;
G_s = specific gravity of solids;
G_{sBENT} = specific gravity of solids for bentonite in GCL;
G_{sGCL} = equivalent specific gravity of solids for GCL;
G_{sGTX} = specific gravity of solids for geotextiles in GCL;
H = thickness of GCL;
H_o = initial thickness of GCL;
h = total hydraulic head;
h_b = total hydraulic head at bottom of GCL;
h_t = total hydraulic head at top of GCL;
K_{dBENT} = distribution coefficient for bentonite in GCL;
K_{dGCL} = equivalent distribution coefficient for GCL;
K_{GML} = partition coefficient for GML;
K_{dGTX} = distribution coefficient for geotextiles in GCL;
k = hydraulic conductivity;
k_o = initial hydraulic conductivity;
M = exponent for effective diffusion coefficient;
M_{BENT} = dry mass of bentonite per unit area of GCL;
M_{GTX} = dry mass of geotextiles per unit area of GCL;
M_e = cumulative contaminant mass outflow per unit area at bottom of GCL;
$M_{e,C}$ = cumulative contaminant mass outflow per unit area for C case;
$M_{e,\mathrm{NC\text{-}I}}$ = cumulative contaminant mass outflow per unit area for NC-I case;
$M_{e,\mathrm{NC\text{-}F}}$ = cumulative contaminant mass outflow per unit area for NC-F case;
MR_F = ratio of cumulative contaminant mass outflow for C case to that for NC-F case;
MR_I = ratio of cumulative contaminant mass outflow for C case to that for NC-I case;
NC-F = simulation that ignores GCL consolidation and uses constant, final conditions of the liner;
NC-I = simulation that ignores GCL consolidation and uses constant, initial conditions of the liner;
n = porosity;
R_f = retardation factor;
q_o = initial vertical effective stress at top of GCL;
s = solid-phase contaminant concentration;
t = time;
t_q = landfill loading period;
v = boundary water outflow rate;
v_s = seepage velocity;
z = elevation;
α_L = longitudinal dispersivity;
γ = moist unit weight of soil;
γ_{sat} = saturated unit weight of soil;
γ_w = unit weight of water;
ΔH = compression of GCL;
Δq = applied vertical stress; and
ρ_w = density of water.

References

ASTM. (2010a). "Standard test methods for liquid limit, plastic limit, and plasticity index of soils." *ASTM D4318*, West Conshohocken, PA.

ASTM. (2010b). "Standard test methods for measurement of hydraulic conductivity of saturated porous materials using a flexible wall permeameter." *ASTM D5084*, West Conshohocken, PA.

ASTM. (2011). "Standard practice for classification of soils for engineering purposes (Unified Soil Classification System)." *ASTM D2487*, West Conshohocken, PA.

Boving, T. B., and Grathwohl, P. (2001). "Tracer diffusion coefficients in sedimentary rocks: Correlation to porosity and hydraulic conductivity." *J. Contam. Hydrol.*, 53(1–2), 85–100.

Castelbaum, D., and Shackelford, C. D. (2009). "Hydraulic conductivity of bentonite slurry mixed sands." *J. Geotech. Geoenviron. Eng.*, 10.1061/(ASCE)GT.1943-5606.0000169, 1941–1956.

Edil, T. B. (2003). "A review of aqueous-phase VOC transport in modern landfill liners." *Waste Manage.*, 23(7), 561–571.

Foose, G. J. (2002). "Transit-time design for diffusion through composite liners." *J. Geotech. Geoenviron. Eng.*, 10.1061/(ASCE)1090-0241(2002)128:7(590), 590–601.

Foose, G. J., Benson, C. H., and Edil, T. B. (2002). "Comparison of solute transport in three composite liners." *J. Geotech. Geoenviron. Eng.*, 10.1061/(ASCE)1090-0241(2002)128:5(391), 391–403.

Fox, P. J. (2007a). "Coupled large strain consolidation and solute transport. I: Model development." *J. Geotech. Geoenviron. Eng.*, 10.1061/(ASCE)1090-0241(2007)133:1(3), 3–15.

Fox, P. J. (2007b). "Coupled large strain consolidation and solute transport. II: Model verification and simulation results." *J. Geotech. Geoenviron. Eng.*, 10.1061/(ASCE)1090-0241(2007)133:1(16), 16–29.

Fox, P. J., and Berles, J. D. (1997). "CS2: A piecewise-linear model for large strain consolidation." *Int. J. Numer. Anal. Methods Geomech.*, 21(7), 453–475.

Fox, P. J., and Lee, J. (2008). "Model for consolidation-induced solute transport with nonlinear and nonequilibrium sorption." *Int. J. Geomech.*, 10.1061/(ASCE)1532-3641(2008)8:3(188), 188–198.

Fox, P. J., and Pu, H. (2012). "Enhanced CS2 model for large strain consolidation." *Int. J. Geomech.*, 10.1061/(ASCE)GM.1943-5622.0000171, 574–583.

Fox, P. J., and Pu, H. (2015). "Benchmark problems for large strain consolidation." *J. Geotech. Geoenviron. Eng.*, 10.1061/(ASCE)GT.1943-5606.0001357, 06015008.

Harpur, W. A., Wilson-Fahmy, R. F., and Koerner, R. M. (1993). "Evaluation of the contact between geosynthetic clay liners and geomembranes in terms of transmissivity." *Proc., 7th GRI Conf. on Geosynthetic Liners Systems: Innovations, Concerns and Design*, Industrial Fabrics Association International, St. Paul, MN, 138–149.

Kang, J.-B., and Shackelford, C. D. (2010). "Consolidation of a geosynthetic clay liner under isotropic states of stress." *J. Geotech. Geoenviron. Eng.*, 10.1061/(ASCE)GT.1943-5606.0000181, 253–259.

Katsumi, T., Ishimori, H., Onikata, M., and Fukagawa, R. (2008). "Long-term barrier performance of modified bentonite materials against sodium and calcium permeant solutions." *Geotext. Geomembr.*, 26(1), 14–30.

Kim, J. Y., Edil, T. B., and Park, J. K. (2001). "Volatile organic compound (VOC) transport through compacted clay." *J. Geotech. Geoenviron. Eng.*, 10.1061/(ASCE)1090-0241(2001)127:2(126), 126–134.

Kolstad, D. C., Benson, C. H., Edil, T. B., and Jo, H. Y. (2004). "Hydraulic conductivity of a dense prehydrated GCL permeated with aggressive inorganic solutions." *Geosynthetics Int.*, 11(3), 233–241.

Lake, C. B. (2000). "Contaminant transport through geosynthetic clay liners and a composite liner system." Ph.D. dissertation, Univ. of Western Ontario, London, ON, Canada.

Lake, C. B., and Rowe, R. K. (2004). "Volatile organic compound diffusion and sorption coefficients for a needle-punched GCL." *Geosynthetics Int.*, 11(4), 257–272.

Lee, J., and Fox, P. J. (2009). "Investigation of consolidation-induced solute transport. II: Experimental and numerical results." *J. Geotech. Geoenviron. Eng.*, 10.1061/(ASCE)GT.1943-5606.0000048, 1239–1253.

Lee, J., Fox, P. J., and Lenhart, J. J. (2009). "Investigation of consolidation-induced solute transport. I: Effect of consolidation on transport parameters." *J. Geotech. Geoenviron. Eng.*, 10.1061/(ASCE)GT.1943-5606.0000047, 1228–1238.

Lee, J.-M., and Shackelford, C. D. (2005). "Concentration dependency of the prehydration effect for a geosynthetic clay liner." *Soils Found.*, 45(4), 27–41.

Lerman, A. (1978). "Chemical exchange across sediment-water interface." *Ann. Rev. Earth Planet. Sci.*, 6, 281–303.

Lewis, T. W., Pivonka, P., Fityus, S. G., and Smith, D. W. (2009). "Parametric sensitivity analysis of coupled mechanical consolidation and contaminant transport through clay barriers." *Comput. Geotech.*, 36(1–2), 31–40.

Malusis, M. A., and Scalia, J. (2007). "Hydraulic conductivity of an activated carbon-amended geosynthetic clay liner." *Proc., Geo-Denver 2007, New Peaks in Geotechnics*, ASCE, Reston, VA, 1–13.

Manheim, F. T. (1970). "The diffusion of ions in unconsolidated sediments." *Earth Planet. Sci. Lett.*, 9(4), 307–309.

Mendes, M. J. A., Touze-Foltz, N., Gardoni, M., Ahari, M., and Mazeas, L. (2013). "Quantification of diffusion of phenolic compounds in virgin GCL and in GCL after contact with a synthetic leachate." *Geotext. Geomembr.*, 38, 16–25.

Mendes, M. J. A., Touze-Foltz, N., Palmeira, E. M., and Pierson, P. (2010). "Influence of the type of bentonite of GCLs on the transmissivity at GCL-geomembrane interfaces." *Proc., 9th Int. Conf. on Geosynthetics, Guaruja, Brazil*, Industrial Fabrics Association International, St. Paul, MN, 919–922.

Mitchell, J. K., et al. (2007). *Assessment of the performance of engineered waste containment barriers*, National Academies Press, Washington, DC.

Othman, M. A., Bonaparte, R., and Gross, B. A. (1997). "Preliminary results of composite liner field performance study." *Geotext. Geomembr.*, 15(4–6), 289–312.

Parker, B. L., Gillham, R. W., and Cherry, J. A. (1994). "Diffusive disappearance of immiscible-phase organic liquids in fractured geologic media." *Ground Water*, 32(5), 805–820.

Peters, G. P., and Smith, D. W. (2002). "Solute transport through a deforming porous medium." *Int. J. Numer. Anal. Methods Geomech.*, 26(7), 683–717.

Pu, H. (2014). "Computational investigations of large strain consolidation and consolidation-induced contaminant transport." Ph.D. dissertation, Univ. of California, San Diego.

Pu, H., and Fox, P. J. (2015). "Consolidation-induced solute transport for constant rate of strain. I: Model development and numerical results." *J. Geotech. Geoenviron. Eng.*, 10.1061/(ASCE)GT.1943-5606.0001171, 04014127.

Pu, H., Fox, P. J., and Shackelford, C. D. (2016). "Assessment of consolidation-induced contaminant transport for compacted clay liner systems." *J. Geotech. Geoenviron. Eng.*, 10.1061/(ASCE)GT.1943-5606.0001426, 04015091.

Rabideau, A., and Khandelwal, A. (1998). "Boundary conditions for modeling transport in vertical barriers." *J. Environ. Eng.*, 10.1061/(ASCE)0733-9372(1998)124:11(1135), 1135–1139.

Rabideau, A. J., et al. (1996). "Contaminant transport modeling (Section 10)." *Assessment of barrier containment technologies*, R. R. Rumer and J. K. Mitchell, eds., National Technical Information Service, Springfield, VA, 247–299.

Sangam, H. P., and Rowe, R. K. (2001). "Migration of dilute aqueous organic pollutants through HDPE geomembranes." *Geotext. Geomembr.*, 19(6), 329–357.

Shackelford, C. D. (1990). "Transit-time design of earthen barriers." *Eng. Geol.*, 29(1), 79–94.

Shackelford, C. D. (2005). "Environmental issues in geotechnical engineering." *16th Int. Conf. on Soil Mechanics and Geotechnical Engineering*, Millpress, Rotterdam, Netherlands, 95–122.

Shackelford, C. D. (2011). *Membrane behavior in geosynthetic clay liners*, ASCE, Reston, VA, 1961–1970.

Shackelford, C. D. (2013). "Membrane behavior in engineered bentonite-based containment barriers: State of the art." *Coupled phenomena in environmental geotechnics*, M. Manassero, A. Dominijanni, S. Foti, and G. Musso, eds., Taylor & Francis Group, London, 45–60.

Shackelford, C. D. (2014). "The ISSMGE Kerry Rowe Lecture: The role of diffusion in environmental geotechnics." *Can. Geotech. J.*, 51(11), 1219–1242.

Shackelford, C. D., Benson, C. H., Katsumi, T., Edil, T. B., and Lin, L. (2000). "Evaluating the hydraulic conductivity of GCLs permeated with non-standard liquids." *Geotext. Geomembr.*, 18(2–4), 133–161.

Sleep, B. E., Shackelford, C. D., and Parker, J. C. (2006). "Modeling of fluid transport through barriers." Chapter 2, *Barrier systems for environmental contaminant containment and treatment*, C. C. Chien, H. I. Inyang, and L. G. Everett, eds., CRC Press, Taylor and Francis Group, London, 71–141.

Ullman, W. J., and Aller, R. C. (1982). "Diffusion coefficients in nearshore marine sediments." *Limnol. Oceanogr.*, 27(3), 552–556.

United States Environmental Protection Agency (U.S. EPA). (2014). "Resource conservation and recovery act orientation manual, chapter III: Managing hazardous waste—RCRA subtitle C." *EPA530-F-11-003*, Washington, DC.

Yaws, C. L. (1995). *Handbook of transport property data*, Gulf Publishing, Houston.

Zekkos, D., et al. (2006). "Unit weight of municipal solid waste." *J. Geotech. Geoenviron. Eng.*, 10.1061/(ASCE)1090-0241(2006)132:10(1250), 1250–1261.

Zhang, H. J., Jeng, D.-S., Barry, D. A., Seymour, B. R., and Li, L. (2013). "Solute transport in nearly saturated porous media under landfill clay liners: A finite deformation approach." *J. Hydrol.*, 479, 189–199.